

This article was downloaded by:

On: 25 January 2011

Access details: Access Details: Free Access

Publisher Taylor & Francis

Informa Ltd Registered in England and Wales Registered Number: 1072954 Registered office: Mortimer House, 37-41 Mortimer Street, London W1T 3JH, UK



Separation Science and Technology

Publication details, including instructions for authors and subscription information:

<http://www.informaworld.com/smpp/title~content=t713708471>

Poly(Acrylic Acid-co-Acrylonitrile) Copolymer Modified Polyethersulfone Hollow Fiber Membrane with pH-Sensitivity

Tao Xiang^a; Qianhao Zhou^a; Kui Li^a; Lulu Li^a; Feifei Su^a; Bosi Qian^a; Changsheng Zhao^{ab}

^a College of Polymer Science and Engineering, State Key Laboratory of Polymer Materials Engineering, Sichuan University, Chengdu, China ^b National Engineering Research Center for Biomaterials, Sichuan University, Chengdu, China

Online publication date: 15 September 2010

To cite this Article Xiang, Tao , Zhou, Qianhao , Li, Kui , Li, Lulu , Su, Feifei , Qian, Bosi and Zhao, Changsheng(2010) 'Poly(Acrylic Acid-co-Acrylonitrile) Copolymer Modified Polyethersulfone Hollow Fiber Membrane with pH-Sensitivity', Separation Science and Technology, 45: 14, 2017 – 2027

To link to this Article: DOI: 10.1080/01496395.2010.504488

URL: <http://dx.doi.org/10.1080/01496395.2010.504488>

PLEASE SCROLL DOWN FOR ARTICLE

Full terms and conditions of use: <http://www.informaworld.com/terms-and-conditions-of-access.pdf>

This article may be used for research, teaching and private study purposes. Any substantial or systematic reproduction, re-distribution, re-selling, loan or sub-licensing, systematic supply or distribution in any form to anyone is expressly forbidden.

The publisher does not give any warranty express or implied or make any representation that the contents will be complete or accurate or up to date. The accuracy of any instructions, formulae and drug doses should be independently verified with primary sources. The publisher shall not be liable for any loss, actions, claims, proceedings, demand or costs or damages whatsoever or howsoever caused arising directly or indirectly in connection with or arising out of the use of this material.

Poly(Acrylic Acid-co-Acrylonitrile) Copolymer Modified Polyethersulfone Hollow Fiber Membrane with pH-Sensitivity

Tao Xiang,¹ Qianhao Zhou,¹ Kui Li,¹ Lulu Li,¹ Feifei Su,¹ Bosi Qian,¹ and Changsheng Zhao^{1,2}

¹College of Polymer Science and Engineering, State Key Laboratory of Polymer Materials Engineering, Sichuan University, Chengdu, China

²National Engineering Research Center for Biomaterials, Sichuan University, Chengdu, China

In this study, functional polyethersulfone (PES) hollow fiber membranes with pH sensitivity were prepared by blending with poly(acrylic acid-co-acrylonitrile) (P(AA-AN)) copolymer. The copolymer was characterized by FTIR analysis, elemental analysis, and GPC measurement. Scanning electron microscopy (SEM) was used to investigate the morphology of the blended hollow fiber membranes. The modified hollow fiber membranes showed excellent pH sensitivity and pH reversibility and we confirmed that both the pore size change and the electroviscous effect had great effect on the pH sensitivity of the copolymer blended PES hollow fiber membranes.

Keywords hollow fiber membrane; pH sensitivity; poly(acrylic acid-co-acrylonitrile); polyethersulfone; ultrafiltration

INTRODUCTION

As new polymeric materials and membranes have been developed in recent years, pH-sensitive membranes have been widely used in drug delivery (1–7) and separation processes (8–15), including salt separation, water purification, separation of ethanol–water solution, and so on.

In the recent decades, many studies have been published for pH-sensitive membranes. Ying et al. (16) prepared microfiltration (MF) membranes from the AAc-g-PVDF copolymers by a phase inversion method. The rate of permeation through the AAc-g-PVDF MF membranes changed reversibly in response to pH variation of the aqueous solutions, and with the most drastic change in permeation rate occurring between pH 2 and 4. Dickson et al. (17) developed the pore-filled pH-sensitive membranes by in situ cross-linking poly(acrylic acid) inside poly(vinylidene

fluoride) (PVDF) hydrophobic microporous substrate membranes and these membranes demonstrated a rapid and reversible response of flux to environmental pH as the pH changed between 2.5 and 7.4.

As we all know, polyethersulfone (PES) is one kind of engineering plastics which possesses the characteristics of wide temperature limits, wide pH tolerances, easy to fabricate many kinds of membranes, wide range of pore sizes distribution available for UF and MF applications, and good chemical resistance to aliphatic hydrocarbons, alcohols, acids, etc. (18). The polymer has been widely used in membrane separation for various applications, such as the microfiltration (MF) and ultrafiltration (UF) process in the fields of biomedicine, food, water purification, etc. (19–24). Nevertheless, the membrane with simple PES could not meet the need of people's demand, so the modifications are urgent to endow PES excellent properties. Such destinations can be achieved by additives to the casting solution and changing the condition of membrane preparation (25–27). On the other hand, surface modification (28–30) is also useful. Our interest is focused on the functionalization of PES membrane to endow it with pH sensitivity, which might have the potential to be used in advanced separation process.

PAA is one of the most important materials having pH sensitivity and ionizable hydrophilic property. According to the study of Hendri (31), the PAA's reversible swelling-shrinking behavior is caused by the transformation between the deionization form (COOH group) and the ionization form (COO[–] group) at pH values around a pKa of about 4.7. However, when PAA was directly blended with the other polymer, the elution of PAA was unavoidable due to its water dissolubility as mentioned in the earlier study (32). According to the binary interaction model, small variations in the molecular structure of one component in blend via copolymerization may lead to large changes in the miscibility of the blends (33). In recent years,

Received 24 October 2009; accepted 20 April 2010.

Address correspondence to Changsheng Zhao, College of Polymer Science and Engineering, State Key Laboratory of Polymer Materials Engineering, Sichuan University, Chengdu, China. Tel.: +86-28-85400453; Fax: +86-28-85405402. E-mail: zhaochsh70@scu.edu.cn

PAN membranes have been attracting much attention in the biomedical fields, since they obviously turn up to be more advantageous over other conventional membranes in various aspects, such as thermal stability, resistance to most organic solvents, atmosphere, bacteria and photo irradiation, commercial availability, etc. (23). Besides, poly(acrylonitrile-co-acrylic acid) was a widely applied copolymer which contains the special property of both the poly(acrylonitrile) and poly(acrylic acid), and it could be easily synthesized (23,25).

In a recent study (34), we provided a simplified method to prepare functional polyethersulfone (PES) membranes with pH-sensitivity and ion exchange capacity by blending cross-linked poly(acrylic acid) (PAA) sub-micrometer-scale gels. We also prepared pH-sensitive polyethersulfone (PES) hollow fiber membranes by blending with a copolymer of acrylonitrile and acrylic acid (PANAA) (35), the copolymer was synthesized by free radical solution polymerization. The blended PES hollow fiber membranes showed excellent pH sensitivity and pH reversibility. We also successfully prepared polyethersulfone-modified montmorillonite hybrid beads for the removal of bisphenol A (36).

In this study, we prepared pH-sensitive PES hollow fiber membranes by blending with poly(acrylic acid-co-acrylonitrile) (P(AA-AN)) copolymer. The copolymer was synthesized by a controlled dosing method via free radical solution polymerization using N-Methyl pyrrolidone (NMP) as the solvent. Through the water flux we investigated the pH sensitivity and pH reversibility of the modified PES hollow fiber membranes. To further explore the effect of pore size change and the electroviscous effect during the separation process, we tested the ultrafiltration of PEG solution. The pore sizes of the membranes under different pH values were calculated, and the pure water permeability was investigated.

EXPERIMENTAL

Materials

Acrylic acid (AA, Kelong Chemical Reagent Company, Chengdu, China) and acrylonitrile (AN; AR) were the monomers to synthesize the P(AA-AN) copolymer. N-methyl pyrrolidone (NMP, Kelong Chemical Reagent Company, Chengdu, China) and Azo-bis-isobutyronitrile (AIBN, Shisihewei Chemical Reagent Company, Shanghai, China) were the solvent and the initiator, respectively. Polyethersulfone (PES, Ultrason E6020P, BASF Aktiengesellschaft) was the polymeric matrix to prepare hollow fiber membrane. Polyethylene glycol (PEG-1000, PEG-4000, PEG-10000), BaCl₂ and I₂ were purchased from Chengdu Kelong Chemical Reagent Company. AN and AA were pretreated by activated carbons before use, and all the other chemicals were used without further purification.

Synthesis of Poly(Acrylic Acid-co-Acrylonitrile) Copolymer

The poly(acrylic acid-co-acrylonitrile) copolymer was synthesized by a controlled dosing method (37) via free radical polymerization in NMP. The monomers were added into the system in three lots with the mass ratio of AA:AN:AA of 30:40:30, and each time the monomers were dissolved in NMP with the monomer concentration of 30%. At first, AA was dissolved in NMP in a three-necked reactor under nitrogen atmosphere for 15 min. When the system arrived at 60°C, AIBN (0.3 wt.% of the total monomers weight) was added and the reaction was carried out for 20 min before starting the addition of AN, and the addition of AN kept for 50 min. And then the rest of the AA was added to the reaction mixture over a period of 50 min. The polymerization was then carried out for 20 h with constant stirring. Then the copolymer was precipitated and washed by double-distilled water several times to remove the residual monomers, initiators, and solvent, which was confirmed by a pH test and UV scanning. The homopolymer of acrylic acid was removed by thoroughly washing with excess ethanol. The copolymer was then dried in a vacuum oven at 60°C for 72 h.

Characterization of the Copolymer

To prepare FTIR samples, the copolymer was dissolved in NMP and cast on a potassium bromide (KBr) disc with the thickness of about 0.8 mm, and then the cast polymer solution was dried by an infrared light. The FTIR spectra were measured with FT-IR Nicolet 560 (Nicol American).

Elemental analysis was performed using a CARLO ERBA 1106 elemental analyzer (Italy), with a carrier gas (He, at a flow rate of 100 ml·min⁻¹) at a combustion temperature of 1000°C using the solid samples. The inverse proportions of C, H, and N were determined.

GPC measurement was performed by using the PL220 GPC analyzer (Britain), and N,N-dimethyl formamide (DMF) was chosen as the eluent.

Preparation of Polyethersulfone Hollow Fiber Membranes and Filters

PES and PANAA copolymer were dissolved in NMP, and the concentration of PES was 18% (wt./wt.). Then the resultant polymer solution was degassed. A dry-wet spinning technique was used to fabricate pH-sensitive polyethersulfone hollow fiber membranes.

The widely used spinning line (38,39) was used for the preparation of the hollow fiber membranes. All the hollow fiber membranes were stored in water bath for 24 h to remove the residual NMP. Afterward, the membranes were post-treated by 50 wt.% glycerol aqueous solution for 24 h to prevent the collapse of porous structures when they were

dried. After drying in air at room temperature, the hollow fiber membranes were used for further test and study.

To test the properties of the hollow fiber membranes in terms of permeation flux and solute sieving coefficient, filters were prepared using epoxy resin as the potting materials. Each filter consisted of 45 hollow fibers, with an effective area of about 120 cm^2 . In this study, three kinds of filters were prepared, namely HFM-18-0, HFM-18-0.8, HFM-18-1.6. HFM-18-0.8 represented that the hollow fiber membranes were prepared from the dope composition of PES and P(AA-AN) with the weight percent of 18% and 0.8%, respectively; and so did the others.

Determination of Ion-Exchange Capacity (IEC)

HCl and NaOH solutions were used to measure the ion-exchange capacity. The hollow fiber membrane filter was alternately equilibrated by 0.1 M HCl and 0.1 M NaOH solutions for several times using the apparatus as mentioned in our earlier study (35), and washed by double-distilled water in between. Afterwards, the filter was circulated by enough NaOH solution with the inlet pressure of 13.3 kPa and outlet pressure of 10.7 kPa, followed by a thorough washing with double-distilled water. Then, the filter was permeated by HCl solution at the same pressure above, and the amount of the HCl was about twice the HCl required for theoretical IEC. The permeated HCl solution was collected and titrated with a standard NaOH solution (0.01 M) by using a pH meter as the indicator. The IEC is expressed in units of milliequivalents of proton atoms per gram of the dried membrane and was calculated by (40):

$$IEC(\text{mequiv./g}) = \frac{V_{\text{HCl}}N_{\text{HCl}} - V_{\text{NaOH}}N_{\text{NaOH}}}{m_c} \times 1000 \quad (1)$$

where V_{HCl} and V_{NaOH} are the volumes of the HCl and NaOH solutions, respectively. N_{HCl} and N_{NaOH} are the normalities of the HCl and NaOH solutions, respectively; and m_c is the weight of dried hollow fiber membranes.

Scanning Electron Microscope (SEM) of the Hollow Fiber Membranes

Scanning electron microscopy (JSM-5900LV, JEOL, Japan) was applied to study the morphology of the hollow fiber membranes. To view the micrographs of the membranes, the membranes were quenched by liquid nitrogen and fractured, coated with a gold layer under vacuum using a sputter apparatus, and then were scanned with the voltage of 20 kV and magnifications of $100\times$ or $500\times$.

The pH Sensitivity Experiment

In our equipment, the equipment for filtration experiments was the same as in our recent study (35). All

the permeability tests were conducted at room temperature and the feed velocity was controlled at 20 ml/min.

At first, pure water was pumped to the hollow fiber filter by a peristaltic pump with inlet pressure of 13.3 kPa and outlet pressure of 10.7 kPa for 1 h to move away the residual glycerol and to get steady state. Then the pH value of the solution changed from 2.0 to 12.0 randomly by adding HCl or NaOH solution, and the permeated solution was collected and the volume was measured. During the process, the flux at each pH value was measured at least 3 times.

The flux was expressed as the hydrodynamic permeability, and calculated by the following equation:

$$Flux(\text{ml}/\text{m}^2 \cdot \text{kPa} \cdot \text{h}) = \frac{V}{S \cdot T \cdot P} \quad (2)$$

where V is the permeate volume; S is the effective membrane area; T is the time of the solution collecting; and P is the pressure applied to the hollow fiber membrane ($P = (13.3 + 10.7)/2 = 12.0\text{ kPa}$, which is the transmembrane pressure).

The pH Reversibility Experiment

The equipment used in this experiment was the same as above. The test filter was pre-compact by aqueous solution with an inlet pressure of 13.3 kPa and an outlet pressure of 10.7 kPa for about 1 hour. Then the filter was alternatively fed by pH 2.5 HCl and pH 11.5 NaOH solutions, and washed by double-distilled water in between. The permeated solution was collected and the fluxes were calculated using Eq. (2).

Ultrafiltration of PEG Solution

The apparatus and test condition were the same as it was in our recent study (35). To study the permeability of polyethylene glycol (PEG) through the membranes, we chose PEG-1000, PEG-4000, and PEG-10000 as the solute. The concentration of the PEG aqueous solution was 100 ppm, which was prepared by dissolving PEG in double-distilled water, and the volume of the solution was 1000 mL. The PEG solution was applied to the membrane by a peristaltic pump with an inlet pressure of 13.3 kPa and an outlet pressure of 10.7 kPa. After reaching the steady state, both the bulk solution and the permeated solution were collected at the same time and the flux was also calculated using Eq. (2). The pH of the PEG solution was changed from 2.0 to 12.0 randomly by adding HCl or NaOH and the filters were washed by double-distilled water after each test so as to move away the residual PEG.

The concentration of the PEG solution was determined by an UV-VIS spectrophotometer (Model 756, Shanghai spectrophotometer instrument Co., Ltd., China). First, the PEG solution reacted with the appropriate amount of

barium chloride solution and iodine solution. Then, the mixed solution was diluted by double-distilled water. In the experiment, the PEG-1000, PEG-4000, PEG-10000 were determined at the wavelength of 661.0 nm, 510.2 nm, and 509.3 nm, respectively.

The observed sieving coefficients (SC_o) were calculated using Eq. (3) as following:

$$SC_o = C_f / C_b \quad (3)$$

where C_f is the filtrate solute concentration; C_b is bulk solute concentration.

RESULTS AND DISCUSSION

Characterization of the Copolymer

The copolymer of P(AA-AN) was synthesized by a controlled dosing method. We added AN and the rest of AA when the conversions ratios were about 70% and 60%, respectively. The percent conversion was measured by weighing the dried polymer using ether as the precipitant. Though the synthesized copolymer could be called block copolymer, it was not a standard block copolymer.

The P(AA-AN) copolymer was characterized using the following tests:

FTIR analysis was measured in the region of 4000–500 cm^{-1} , as shown in Fig. 1. It can be seen that the peaks at 1406 cm^{-1} , 1731 cm^{-1} , and 1261 cm^{-1} were the characteristic peaks of the –OH, C=O, and –C–O– in the carboxyl group of AA, respectively. The peak at 2241 cm^{-1} could attribute to the –CN of the AN chains in the copolymer. Furthermore, the peaks at 2929 cm^{-1} and 1451 cm^{-1} could attribute to the –CH₂– and –CH– in the trunk chain of the copolymer, respectively. The

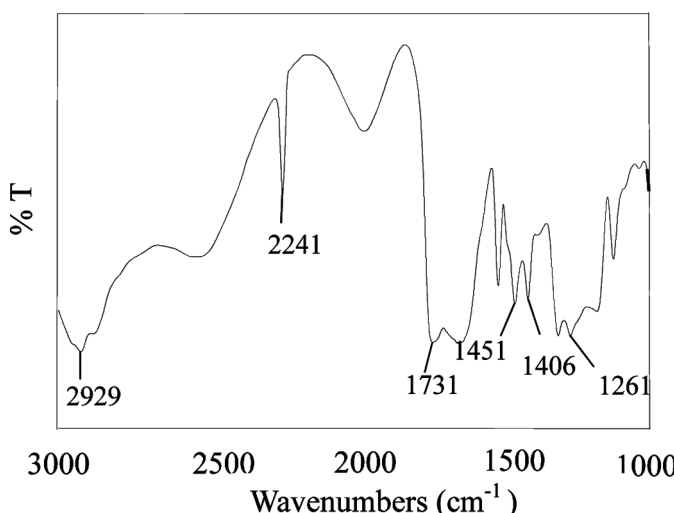


FIG. 1. FTIR spectra of P(AA-AN-AA) block copolymer.

FTIR spectra indicated that the copolymer of PAA-AN was synthesized.

Elemental analysis, which is based on the determination of carbon (C), hydrogen (H) and nitrogen (N), was performed using an elemental analyzer. From the elemental analysis data, the weight ratio of AA to AN in the copolymer chains could be calculated with 54.28:45.72, which approached the ratio of the monomers used in the polymerization 60:40.

GPC measurement is performed to determine the molecular weight of the copolymer which was calibrated with polystyrene as the standard polymer. The number-average molecular weight (M_n), weight-average molecular weight (M_w), and Z-average molecular weight (M_z) are 3.2×10^4 , 12.31×10^4 , and 54.32×10^4 , respectively.

SEM of the Hollow Fiber Membrane

Scanning electron microscopy (SEM) was used to investigate the structure and morphology of the hollow fiber membranes. We took micrographs of the cross-sections, inner and out surfaces of the hollow fiber membranes. However, the micrographs of both inner and outer surfaces showed no significant difference for different membranes. The SEM pictures of the cross-sections of the membranes are shown in Fig. 2. As shown in Fig. 2, the wall thickness of the hollow fiber membrane was about 80 μm and the inner-diameter was about 600 μm . A skin layer could be found on both sides of the membrane wall, between which were a finger-like structure and the porous structure, which was in accordance with the other report (41). The existing of double skin layers can influence the molecular orientation on the outer surface of the membranes, which directly affect the membrane separation performance. Furthermore, it was observed that the finger-like structure was not in the middle of the membrane and the morphology of the two skin layers was different. These were mainly related to the dry-wet spinning method. In the preparation process of hollow fiber membranes, the exchange between NMP and water occurred from the inner side of the nascent fiber when the spinning dope was extruded through the spinneret. Then the exchange occurred from the outside when the nascent fiber got in the coagulation bath. In this case, a porous structure formed in the middle of the hollow membrane. There are obvious differences among the three samples as shown in Fig. 2. After blending the P(AA-AN) copolymer, the size of the finger-like cavities in the membranes decreased, and many small pores were observed near the finger-like structure.

Ion Exchange Capacity (IEC)

To investigate the charge property of the blended membrane, the ion exchange capacity (IEC) of the membrane was studied. The calculated IECs for the membrane HFM-18-0.8 and HFM-18-1.6 were 0.32 mequiv./g and

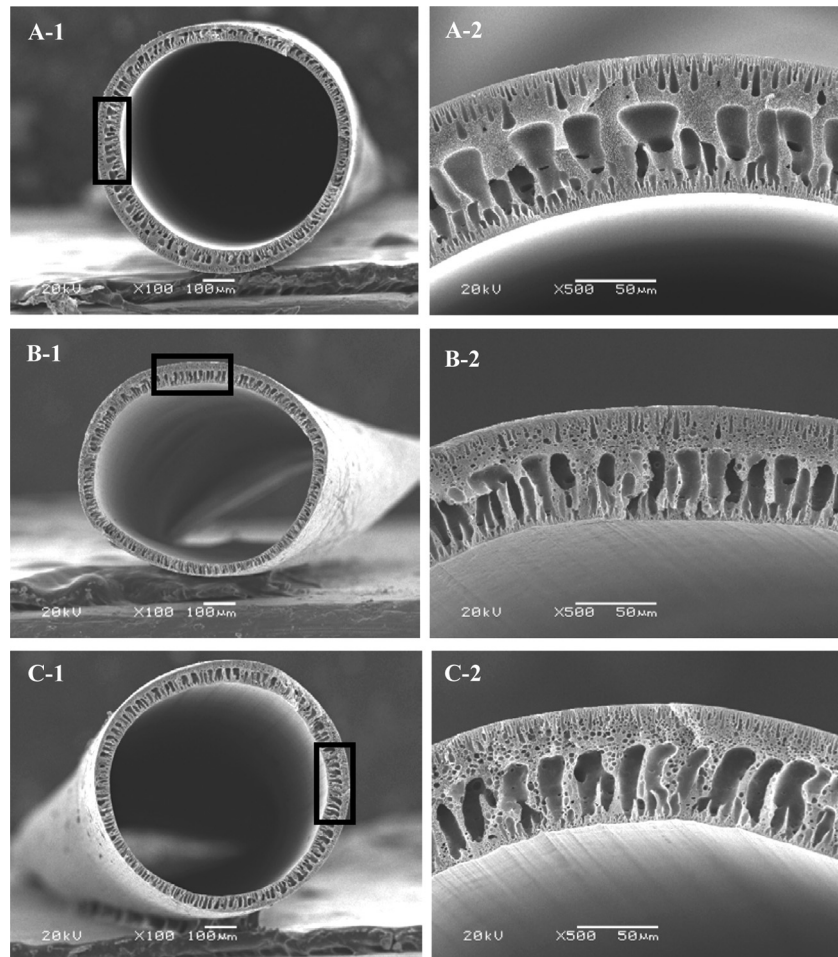


FIG. 2. SEM images of the cross-section views of the membranes HFM-18-0 (A-1 and A-2), HFM-18-0.8 (B-1 and B-2) and HFM-18-1.6 (C-1 and C-2). Magnification: (A-C-1) 100 \times ; (A-C-2) 500 \times .

0.62 mequiv./g, respectively compared with the titrated IECs of the two fibers which were 0.29 mequiv./g and 0.55 mequiv./g, respectively, and these were about 90% of the calculated IECs. The titrated IECs were slightly smaller than the calculated IECs. When the membranes were equilibrated in the NaOH solution, the ionized carboxyl groups diminished the tendency of their neighbors to ionize. According to the article (42), the IECs of the commercial iron exchange membranes are 1–2 mequiv./g, thus the prepared hollow fiber membranes could not be used as ion exchange membranes. Nevertheless, their characteristic of pH sensitivity was notable, which will be discussed in the following sections.

Membrane Water Flux as a Function of pH Value

The effect of pH value on water flux through the three filters (HFM-18-0, HFM-18-0.8, and HFM-18-1.6) was studied and the results are presented in Fig. 3. As shown in the figure, when the pH values changed from 2.0 to 12.0, the water flux for the HFM-18-0 filters was not

changed, which was about $700.8 \text{ ml}/(\text{m}^2 \cdot \text{kPa} \cdot \text{h})$. However, the fluxes for HFM-18-0.8 and HFM-18-1.6 decreased. The fluxes for HFM-18-0.8 decreased from 834.7 to $127.1 \text{ ml}/(\text{m}^2 \cdot \text{kPa} \cdot \text{h})$, and the flux change was about 6.5 times; while those decreased from 1094.2 to $206.8 \text{ ml}/(\text{m}^2 \cdot \text{kPa} \cdot \text{h})$ for the HFM-18-1.6, and the flux change was about 5.3 times. Furthermore, with the increase of copolymer concentration, the flux increased at the same pH. This may be caused by the increased hydrophilicity and the pore size change. During the process, when the filter got to the steady state, the flux hardly changed. It should be noticed that the filter could be used for many times if it was immersed in water, and flux had no obvious change.

The water fluxes of the hollow fiber membranes exhibited chemical valve behavior at pH between 6.0 and 11.0 for HFM-18-0.8; and between 4.5 and 11.0 for HFM-18-1.6. The water fluxes hardly changed at the pH value lower than 6.0 for HFM-18-0.8 and lower than 4.5 for HFM-18-1.6, respectively. It is reported that the pKa

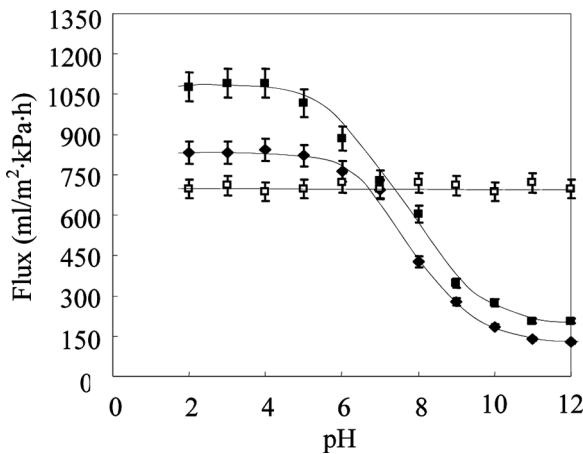


FIG. 3. Water flux as a function of pH values. For the membrane: HFM-18-0 (□); HFM-18-0.8 (◆); HFM-18-1.6 (■). Duplicate experiments showed similar results.

of PAA in solution is about 4.3–4.9 dependent upon the measurement method (43,44), which is not in agreement with that from Fig. 3. These might be caused by the change of the PAA molecular chain morphology in the block copolymer, and the AN chain might also affect the dissociation of $-\text{COOH}$.

Membrane pH Reversibility

To study the membrane flux as a function of environmental pH, the pH reversibility of the membrane was evaluated by the buffer solution flux at pH 2.5 and 11.5, data are presented in Fig. 4. Each experimental run involved 10 min equilibration in the solution flow followed by 10 min sample collecting. As shown in the figure, when

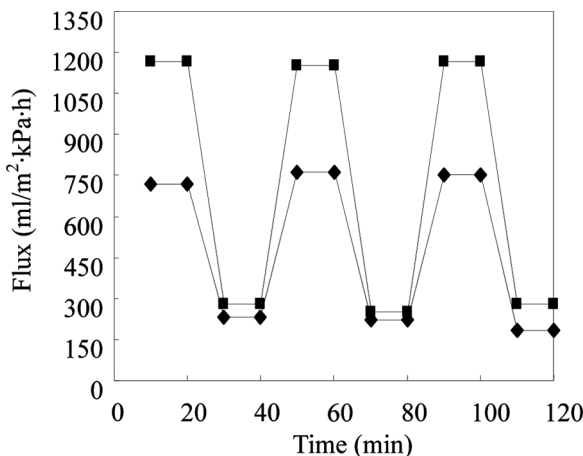


FIG. 4. Water flux for the membrane as the feed was exchanged between pH 2.5 and 11.5 with 10 min equilibration flow followed by 10 min sample collecting. For the membranes: HFM-18-0.8 (◆); HFM-18-1.6 (■). Duplicate experiments showed similar results.

the solution was alternated, the fluxes were reversible between about 750.0 and 218.1 $\text{mL}/(\text{m}^2 \cdot \text{kPa} \cdot \text{h})$ for HFM-18-0.8, and 1165.6 and 278.2 $\text{mL}/(\text{m}^2 \cdot \text{kPa} \cdot \text{h})$ for HFM-18-1.6, respectively. At pH 11.5, the carboxylic acids of PAA can dissociate to carboxylate ions to provide high charge density in the membranes, and the P(AA-AN) copolymer would be swelling. Thus the water flux was small at pH 11.5. The permeability change was about 3.4 times for the HFM-18-0.8 membrane; while that permeability change was 4.2 times for the HFM-18-1.6 membrane. It was found that the fluxes change was not proportional to the copolymer amount. These indicated that the flux change was affected not only by the membrane charge density or electroviscous effect, but also the pore size of the membrane, which will be discussed in the next section.

Membrane Pore Size Determined by Solute Sieving Coefficients

To further investigate the effect of pore size change and the electroviscous effect on the pH sensitivity, the pore size of the membranes was determined based on a hydrodynamic model (45–49).

According to the classical hydrodynamic model, the so called “pore model,” the pore size of the hollow fiber membrane could be calculated using the following equation:

$$SC_a = C_f / C_m = 2(1 - q)^2 - (1 - q)^4 \quad (4)$$

where SC_a is the actual coefficient; C_f is the filtrate solute concentration; C_m is solute concentration at the membrane; q is the radius ratio of the solute (r_s) to the membrane pore (r_p), $q = r_s / r_p$. The radius (r_s) of the solute in solution could be calculated by the equation (50), $r_s = (3M / 4\pi\rho N)^{1/3}$, where M is the molecular weight, ρ is the density, and N is the Avogadro's number. The calculated radius for PEG-4000 and PEG-10000 were 11.7 and 15.8 Å, respectively.

The actual sieving coefficients (SC_a) could be evaluated from the experimental data for the observed sieving coefficients (SC_o) using the following equation based on a stagnant film model (51,52):

$$SC_a = \frac{SC_o}{(1 - SC_o) \exp(J_v/k) + SC_o} \quad (5)$$

where K is the mass transfer coefficients, J_v is the volumetric filtrate flux (volume flow rate per membrane area).

Due to the concentration polarization, the actual sieving coefficient was smaller than the observed sieving coefficient, while the actual rejection coefficient was larger than the observed rejection coefficient. According to our recent study (35), at high shear rate for a small molecular weight

solute PEG (53,54), the concentration polarization was not obvious at the experimental conditions. And there was no obvious difference between the actual rejection coefficients and the observed rejection coefficients. Thus, the observed sieving coefficients (SC_o) could be used directly to calculate the pore size.

Figure 5 shows the effect of pH values on the observed sieving coefficients. As shown in the figure, for HFM-18-0 membrane, the observed sieving coefficients ranged from 0.47 to 0.50 and changed little when PEG-4000 solution changed from basic to acid condition; for the HFM-18-0.8 membrane, those ranged from 0.46 to 0.79 when PEG-4000 solution changed from basic to acid condition; for the HFM-18-1.6, those ranged from 0.41 to 0.74 when PEG-10000 solution changed from basic to acid condition. Here PEG-10000 was used to evaluate HFM-18-1.6, since the molecular weight of PEG-4000 was relatively small. In fact, for each membrane, PEG-1000, PEG-4000, and PEG-10000 were used to determine the pore size, though the observed sieving coefficients showed significant differences, the calculated pore sizes showed no significant differences. The calculated pore size for the HFM-18-0 was 2.55 nm. The calculated pore sizes of the membranes (HFM-18-0.8 and HFM-18-1.6) and the hydrodynamic permeability for the PEG solution are shown in Fig. 6. Furthermore, during the test process, the sieving coefficient hardly changed along with the operating time.

As shown in Fig. 6, both the pore size and the flux decreased when the PEG solution changed from acid to

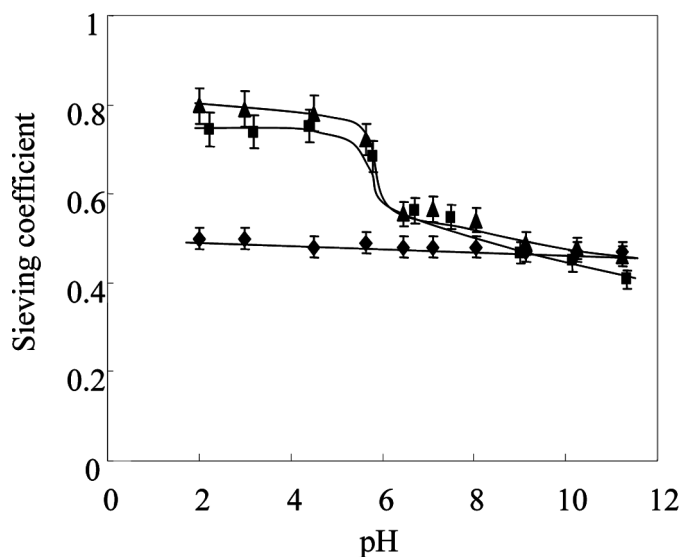


FIG. 5. Sieving coefficient at different pH values. For the membrane: HFM-18-0 (◆), and PEG-4000 solution was used; HFM-18-0.8 (▲), and PEG-4000 solution was used; HFM-18-1.6 (■), and PEG-10000 solution was used.

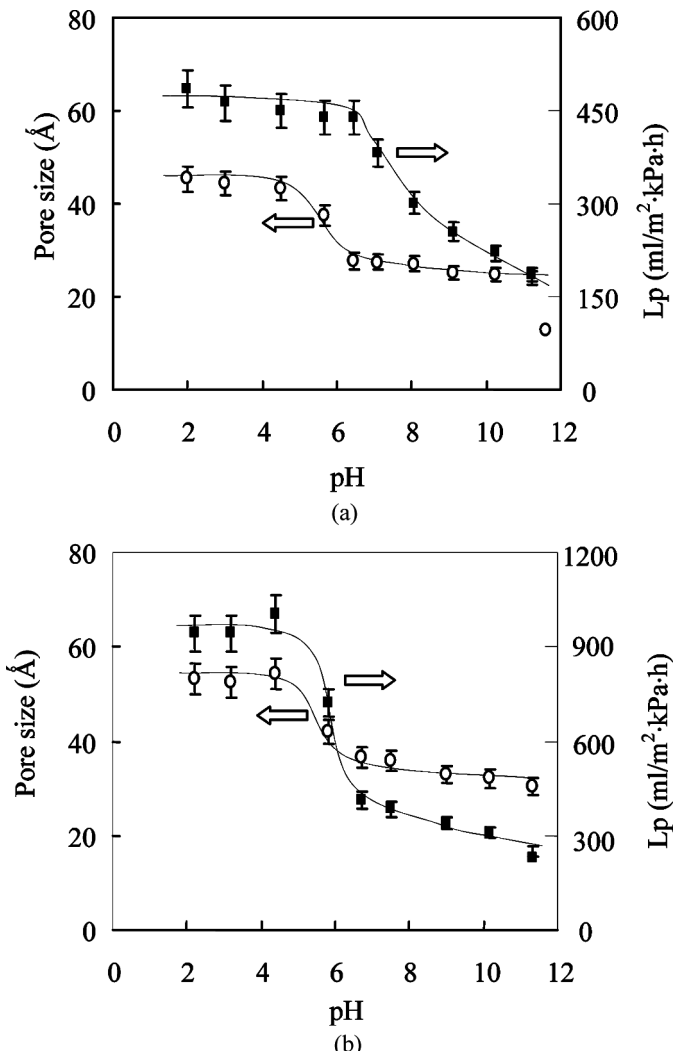


FIG. 6. Flux change and the calculated pore size for the membranes at different pH values; Pore size: (○); permeability of PEG solution (■). (a) is for the HFM-18-0.8 filter, and PEG-4000 solution was used; (b) is for the HFM-18-1.6 filter, and PEG-10000 solution was used.

basic condition. However, the decrease tendency was different for the two membranes. For the membrane HFM-18-0.8, the flux of PEG-4000 solution had no change at the pH values ranged from 2 to 6.5; when the pH value was larger than 6.5, the flux decreased gradually. The pore size had a sharp decrease at the pH values of 4.5 to 6.5, and hardly changed at the pH value lowered than 4.5 and exceeded 6.5. For the membrane HFM-18-1.6, the flux of PEG-10000 solution exhibited chemical valve behavior at pH between 4.5 and 6.5, and hardly changed at the pH value lowered than 4.5; when the pH value was larger than 6.5, the flux decreased gradually. The pore size for membrane HFM-18-1.6 also had a sharp decrease at the pH between 4.5 and 6.5, and hardly changed at pH value lowered than 4.5 and exceeded 6.5.

It is interesting to note that the pH values for the pore size change of the two kinds of membranes ranged between 4.5 and 6.5, though the flux change might not be in this range. As is known, the chain configuration of weak polyacid is a function of pK_a of the polymer. The pK_a of PAA in solution is about 4.3–4.9 dependent upon the measurement method (42,43), which is in agreement with the pore size change as shown in Fig. 6. These results suggested that the pore size change was caused by the ionization of the copolymerized PAA, and the pH value of the ionization did not change even in the copolymers. The flux change was not in agreement with the pore size change for membrane HFM-18-0.8, but the same as for membrane HFM-18-1.6. These results indicated that both the pore size change and the electroviscous effect had great effect on the flux change, and their effect on different membranes was different, and these will be further discussed in the next section.

Effect of Pore Size Change and Electroviscous Effect on Water Permeability

To further investigate the effect of pore size change and electroviscous effect on permeability, the water permeability should be calculated based on the pore size calculated above.

The principle of the water permeability method to determine membrane pore size is the capillary pore diffusion model and the Hagan-Poiseuille equation, and the mean pore radius can be calculated by the following equation (46):

$$r = (8\mu A_x L_p / A_k)^{1/2} \quad (6)$$

where μ is the viscosity of water, A_x the membrane thickness, A_k the membrane surface porosity, and L_p is the hydraulic permeability. Thus, the pure water permeability (PWP) could be calculated using the transformation of the equation above, and expressed as following.

$$L_p = r^2 A_k / 8\mu A_x \quad (8)$$

To calculate the hydraulic permeability, the membrane surface porosity should be calculated, since the viscosity of water (μ) and the membrane thickness (A_x) are constants. Assume the membrane surface porosity (A_k) is a constant, and does not change with the pH variation. The porosity (A_k) could be calculated using the radius (r) calculated from the sieving coefficient at the pH = 7.0 and the corresponding pure water permeability. Thus, the PWP of the hollow fiber membranes at the corresponding radius (at different pH values) could be calculated, as shown in Fig. 7. It should be noticed that the pure water permeability was not the flux at the corresponding pH

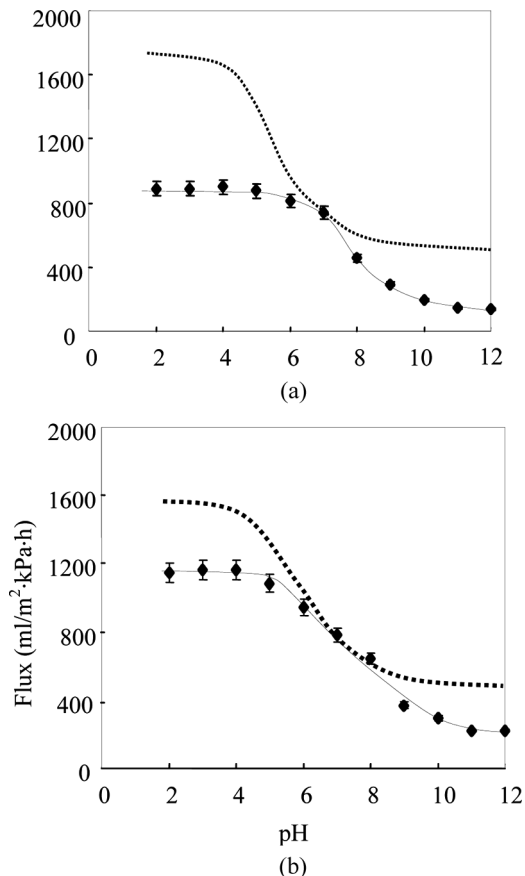


FIG. 7. Experimental flux and the pure water permeability calculated from the pore size; The real line is for the experimental flux; the broken line is for the calculated pure water permeability. (a) is for the HFM-18-0.8 filter; (b) is for the HFM-18-1.6 filter.

values, but the flux at the corresponding radius when the membranes had no charge.

As shown in the figure, the corresponding pure water permeability was larger than the experimental flux for the two kinds of membranes both at the acid and basic conditions. These were caused by the electroviscous effect. For the non-charged membrane, such as the PES membrane, there is no change in the permeability when the solution changed from acid to basic condition. However, for the charged membranes, such as for the HFM-18-0.8 or HFM-18-1.6, the membrane had charge or the charge density was very small at acid condition, but the solution had negative charges, thus the flux decreased. At the basic condition, the pore size had no change as indicated from the pure water permeability in the figure and mentioned above, the membrane charge density increased, thus the flux decreased. These results indicated that the electroviscous effect had great effect on the hydrodynamic permeability, which was conformable with the electroviscous effect theory.

Compared to the data in Fig. 7(a) and 7(b), it should be noticed that the difference between the calculated pure water permeability and experimental flux for HFM-18-1.6 was smaller than that for HFM-18-0.8. This suggested that the electroviscous effect on membrane HFM-18-1.6 was smaller than that on HFM-18-0.8. As mentioned above, the pore size for membrane HFM-18-1.6 was larger than that for membrane HFM-18-0.8. These indicated that when the pore size of the charged membrane was small, the electroviscous effect was strong. For the large pore size charged membrane, the flux change was mainly caused by the pore size change, not by the electroviscous effect.

CONCLUSION

Poly(acrylic acid-co-acrylonitrile) (P(AA-AN)) copolymer with nonstandard block structure was synthesized by a controlled dosing method via free radical solution polymerization. And by blending P(AA-AN) copolymer with PES, functional polyethersulfone hollow fiber membranes were successfully prepared. The membranes demonstrated significant pH sensitivity and pH reversibility due to the AA chains. And with the increase of the copolymer amount, the flux increased. Furthermore, we measured the pore size of the membrane through the ultrafiltration of the PEG solution. The results indicated that when the pore size was small, the electroviscous effect was strong; however, when the pore size was very large, the flux change was mainly caused by the pore size change, not by the electroviscous effect. What is more, the prepared hollow fiber filter may be widely used in special separating process due to its pH sensitivity.

ACKNOWLEDGEMENTS

This work was financially sponsored by the National Natural Science Foundation of China (No. 50673064), State Education Ministry of China (Doctoral Program for High Education, No. JS20061116506327), and Sichuan Youth Science and Technology Foundation (08ZQ026-038). We would also like to thank our laboratory members for their generous help, and gratefully acknowledge the help of Ms. X.Y. Zhang and Ms. H. Wang of the Analytical and Testing Center at Sichuan University, for the SEM micrographs.

LIST OF SYMBOLS

Nomenclature

A_x	the membrane thickness (μm)
A_k	the membrane surface porosity
C_b	bulk solute concentration (mol/L)
C_f	filtrate solute concentration (mol/L)
C_m	the solute concentration at the membrane (mol/L)
$Flux$	the hydrodynamic permeability ($\text{ml}/\text{m}^2 \cdot \text{mmHg} \cdot \text{h}$)

J_v	the volumetric filtrate flux
K	the mass transfer coefficient
L_p	the hydraulic permeability ($\text{ml}/\text{m}^2 \cdot \text{mmHg} \cdot \text{h}$)
M	the molecular weight (g/mol)
mc	the weight of dried hollow fiber membrane (g)
N	the Avogadro's number
N_{HCl}	normality of the HCl and NaOH solutions (N)
N_{NaOH}	normality of the HCl and NaOH solutions (N)
P	pressure applied to the hollow fiber membrane (kPa)
q	radius ratio of the solute (r_s) to the membrane pore (r_p)
S	the effective membrane area (m^2)
SC_a	actual sieving coefficient
SC_o	observed sieving coefficient
T	the time of the solution collecting (h)
V	the permeate volume (ml)
V_{HCl}	the volume of the HCl solution (L)
V_{NaOH}	the volume of the NaOH solution (L)
C_m	the solute concentration at the membrane (mol/L)

Greek Letters

ρ	the density (g/cm^3)
μ	the viscosity of water ($\text{Pa} \cdot \text{s}$)

REFERENCES

- Li, F.; Liu, W.G.; Yao, K.D. (2002) Preparation of oxidized glucose-crosslinked N-alkylated chitosan membrane and in vitro studies of pH-sensitive drug delivery behaviour. *Biomaterials*, 23 (2): 343-347.
- Drummond, D.C.; Zignani, M.; Leroux, J.C. (2000) Current status of pH-sensitive liposomes in drug delivery. *Prog. Lipid. Res.*, 39 (5): 409-460.
- Park, S.B.; You, J.O.; Park, H.Y.; Haam, S.J.; Kim, W.S. (2001) A novel pH-sensitive membrane from chitosan -TEOS IPN; preparation and its drug permeation characteristics. *Biomaterials*, 22 (4): 323-330.
- Kyriakides, T.R.; Cheung, C.Y.; Murthy, N.; Bornstein, P.; Stayton, P.S.; Hoffman, A.S. (2002) pH-Sensitive polymers that enhance intracellular drug delivery in vivo. *J. Control. Release.*, 78 (1-3): 295-303.
- Shieh, M.J.; Lai, P.S.; Young, T.H. (2002) 5-Aminosalicylic acid permeability enhancement by a pH-sensitive EVAL membrane. *J. Membr. Sci.*, 204 (1/2): 237-246.
- Mrsny, R.J. (1992) The colon as a site for drug delivery. *J. Control. Release.*, 22 (1): 15-34.
- Watts, P.J.; Llum, L. (1997) Colonic drug delivery. *Drug Dev. Ind. Pharm.*, 23 (9): 893-913.
- Berezina, N.P.; Kononenko, N.A.; Dyomina, O.A.; Gnusin, N.P. (2008) Characterization of ion-exchange membrane materials: Properties vs structure. *Adv. Colloid. Interfac.*, 139: 3-28.
- Bandini, S.; Drei, J.; Vezzani, D. (2005) The role of pH and concentration on the ion rejection in polyamide nanofiltration membranes. *J. Membr. Sci.*, 264 (1/2): 65-74.

10. Hsueh, C.L.; Kuo, J.F.; Huang, Y.H.; Wang, C.C.; Chen, C.Y. (2005) Separation of ethanol–water solution by poly(acrylonitrile-co-acrylic acid) membranes. *Sep. Purif. Technol.*, 41 (1): 39–47.
11. Mika, A.M.; Childs, R.F.; Dickson, J.M. (2002) Salt separation and hydrodynamic permeability of a porous membrane filled with pH-sensitive gel. *J. Membr. Sci.*, 206: 19–30.
12. Solpan, D.; Sahan, M. (1998) The separation of Cu²⁺ and Ni²⁺ from Fe³⁺ ions by complexation with alginic acid and using a suitable membrane. *Separ. Sci. Technol.*, 33 (6): 909–914.
13. Zhao, C.S.; Wei, Q.R.; Yang, K.G.; Liu, X.D.; Nomizu, M.; Nishi, N. (2004) Preparation of porous polysulfone beads for selective removal of endocrine disruptors. *Separ. Sci. Technol.*, 40 (3): 297–302.
14. Zhao, C.S.; Liu, X.D.; Nomizu, M.; Nishi, N. (2004) Preparation of DNA-loaded polysulfone microspheres by liquid-liquid phase separation and its functional utilization. *J. Colloid. Interf. Sci.*, 275 (2): 470.
15. Strathmann, H. (2001) Membrane separation processes: Current relevance and future opportunities. *Aiche. J.*, 47 (5): 1077–1087.
16. Ying, L.; Wang, P.; Kang, E.T.; Neoh, K.G. (2002) Synthesis and characterization of poly(acrylic acid)-graft-poly(vinylidene fluoride) copolymers and pH-sensitive membranes. *Macromolecules*, 35 (3): 673–679.
17. Hu, K.; Dickson, J.M. (2007) Development and characterization of poly(vinylidene fluoride)-poly(acrylic acid) pore-filled pH-sensitive membranes. *J. Membr. Sci.*, 301 (1/2): 19–28.
18. Cheryan, M. (1998) *Ultrafiltration and Microfiltration Handbook*; Technomic Publishing Co.: Lancaster, PA.
19. Pontié, M.; Durand-Bourlier, L.; Lemordant, D.; Lainé, J.M. (1998) Control fouling and cleaning procedures of UF membranes by a streaming potential method. *Sep. Purif. Technol.*, 14 (1–3): 1–11.
20. David, S.; Gerra, D.; De Nitti, C.; Bussolati, B.U.; Teatini, G.R.; Longhena, C.; Guastoni, N.; Bellotti, F.; Combarnous, C.; Tetta, A. (2003) Hemodialfiltration and high-flux hemodialysis with polyether-sulfone membranes. *Contrib. Nephrol.*, 138: 43–54.
21. Zhao, C.S.; Yu, B.Y.; Qian, B.S.; Wei, Q.; Yang, K.G.; Zhang, A.M. (2008) BPA transfer rate increase using molecular imprinted polyethersulfone hollow fiber membrane. *J. Membr. Sci.*, 310 (1/2): 38–43.
22. Wienk, I.M.; Teunis, H.A.; Boomgaard, Th.v.d.; Smolders, C.A. (1993) A new spinning technique for hollow fiber ultrafiltration membranes. *J. Membr. Sci.*, 78 (1/2): 93–100.
23. Wang, Z.G.; Wan, L.S.; Xu, Z.K. (2007) Surface engineerings of polyacrylonitrile-based asymmetric membranes towards biomedical applications: An overview. *J. Membr. Sci.*, 304 (1/2): 8–23.
24. Suman, M.; Debashis, R.; Pinaki, B. (2008) Affinity separation of trypsin from goat pancreatic extract using a polyethersulfone ultrafiltration membrane. *Separ. Sci. Technol.*, 43 (11/12): 3333–3350.
25. Ismail, A.F.; Hassan, A.R. (2007) Effect of additive contents on the performances and structural properties of asymmetric polyethersulfone (PES) nanofiltration membranes. *Sep. Purif. Technol.*, 55 (1): 98–109.
26. Boom, R.M.; van den Boomgaard, T.; Smolders, C.A. (1994) Mass transfer and thermodynamics during immersion precipitation for a two-polymer system: Evaluation with the system PES–PVP–NMP–water. *J. Membr. Sci.*, 90 (3): 231–249.
27. Lafreniere, L.Y.; Talbot, D.F.; Matsuura, T.; Sourirajan, S. (1987) Effect of polyvinylpyrrolidone additive on the performance of polyethersulfone ultrafiltration membranes. *Ind. Eng. Chem. Res.*, 26 (11): 2385–2389.
28. Rana, D.; Matsuura, T.; Narbaitz, R.M.; Feng, C. (2005) Development and characterization of novel hydrophilic surface modifying macromolecule for polymeric membranes. *J. Membr. Sci.*, 249 (1/2): 103–112.
29. Fang, B.H.; Ling, Q.Y.; Zhao, W.F.; Ma, Y.L.; Bai, P.L.; Wei, Q.; Li, H.F.; Zhao, C.S. (2009) Modification of polyethersulfone membrane by grafting bovine serum albumin on the surface of polyethersulfone/poly(acrylonitrile-co-acrylic acid) blended membrane. *J. Membr. Sci.*, 329 (1/2): 46–55.
30. Kouwonou, Y.; Malaisamy, R.; Jones, K.L. (2008) Modification of PES membrane: Reduction of biofouling and improved flux recovery. *Separ. Sci. Technol.*, 43 (16): 4099–4112.
31. Hendri, J.; Hiroki, A.; Maekawa, Y.; Yoshida, M.; Katai, R. (2001) Permeability control of metal ions using temperature- and pH-sensitive gel membranes. *Radiat. Phys. Chem.*, 60 (6): 617–624.
32. M'Barek, C.O.; Nguyen, Q.T.; Alexandre, S.; Zimmerlin, I. (2006) Fabrication of ion-exchange ultrafiltration membranes for water treatment: I. Semi-interpenetrating polymer networks of polysulfone and poly(acrylic acid). *J. Membr. Sci.*, 278 (1/2): 10–18.
33. Paul, D.R.; Bucknall, C.B. (1999) *Polymer Blends*; John Wiley & Sons, New York.
34. Wei, Q.; Li, J.; Qian, B.S.; Fang, B.H.; Zhao, C.S. (2009) Preparation characterization and application of functional polyethersulfone membranes blended with poly(acrylic acid) gels. *J. Membr. Sci.*, 337 (1/2): 266–273.
35. Qian, B.S.; Li, J.; Wei, Q.; Bai, P.L.; Fang, B.H.; Zhao, C.S. (2009) Preparation and characterization of pH-sensitive polyethersulfone hollow fiber membrane for flux control. *J. Membr. Sci.*, 344 (1/2): 297–303.
36. Yin, C.; Chen, T.; Cao, F.M.; Yin, Z.H.; He, X.J.; Jian, G.; Zhang, A.Q.; Zhao, C.S. (2008) Polyethersulfone-modified montmorillonite hybrid beads for the removal of bisphenol A. *Separ. Sci. Technol.*, 43 (6): 1404–1420.
37. Sahoo, A.; Jassal, M.; Agrawa, A.K. (2008) pH-responsive fibers based on acrylonitrile acrylic acid block copolymers: Effect of spinning conditions and postspinning operations on response and mechanical properties. *J. Appl. Polym. Sci.*, 109 (6): 3792–3803.
38. Chung, T.S.; Qin, J.J.; Gu, J. (2000) Effect of shear rate within the spinneret on morphology, separation performance and mechanical properties of ultrafiltration polyethersulfone hollow fiber membranes. *Chem. Eng. Sci.*, 55 (6): 1077–1091.
39. Chung, T.S.; Kafchinski, E.R. (1997) The Effects of spinning conditions on asymmetric 6FDA/6FDAM polyimide hollow fibers for air separation. *J. Appl. Polym. Sci.*, 65 (8): 1555–1569.
40. Mika, A.M.; Childs, R.F.; Dickson, J.M.; McCarry, B.E.; Gagnon, D.R. (1995) A new class of polyelectrolyte-filled microfiltration membranes with environmentally controlled porosity. *J. Membr. Sci.*, 108: 37–56.
41. Qin, J.J.; Gu, J.; Chung, T.S. (2001) Effect of wet and dry-jet wet spinning on the shear-induced orientation during the formation of ultrafiltration hollow fiber membranes. *J. Membr. Sci.*, 182 (1/2): 57–75.
42. Strathmann, H. (1991) Electrodialysis. In: *Membrane Separation Systems: Recent Developments and Future Directions*, Baker, R.W.; Cussler, E.L.; Eykamp, W.; Koros, W.J.; Riley, R.L.; Strathmann, H., eds.; Noyes Data Corp.: Park Ridge.
43. Mark, H.; Gaylord, N.; Bikales, N. (1976) *Encyclopedia of Polymer Science and Technology*; Interscience Publishers.
44. Rollefson, G.; Powell, R. (1952) *Annual Review of Physical Chemistry*, vol. 3, *Annual Review*; Inc.: Stanford, CA.
45. Zhao, C.S.; Zhou, X.S.; Yue, Y.L. (2000) Determination of pore size and pore size distribution on the surface of hollow-fiber filtration membranes: A review of methods. *Desalination*, 129 (20): 107–123.
46. Ravikovich, P.I.; Haller, G.L.; Neimark, A.V. (1998) Ensite functional theory model for calculating pore size distributions: Pore structure of nanoporous catalysts. *Adv. Colloid Interface Sci.*, 76–77: 203–226.
47. Ferry, J.D. (1936) Statistical evaluation of sieve constants in ultrafiltration. *J. Gen. Physiol.*, 20 (1): 95–104.
48. Verniory, A.; Bois, R.D.; Decoedt, P.; Gassee, J.P.; Lambert, P.P. (1973) Measurement of the permeability of biological membranes. Applications to the glomerular wall. *J. Gen. Physiol.*, 62 (4): 489–507.

49. Haberman, W.L.; Sayre, R.M. (1958) Motion of rigid and fluid spheres in stationary and moving liquids inside cylindrical tubes. David Taylor Modes Basin Report, Department of the Navy: US.

50. Durbin, R.P. (1960) Osmotic flow of water across permeable cellulose membranes. *J. Gen. Physiol.*, 44 (2): 315–326.

51. Zeman, L.J.; Zydny, A.L. (1996) *Microfiltration and Ultrafiltration: Principles and Applications*; Marcel Dekker Inc.: New York.

52. Mehta, A.; Zydny, A.L. (2005) Permeability and selectivity analysis for ultrafiltration membranes. *J. Membr. Sci.*, 249 (1/2): 245–249.

53. Bian, R.; Yamamoto, K.; Watanabe, Y. (2000) The effect of shear rate on controlling the concentration polarization and membrane fouling. *Desalination*, 131 (1–3): 225–236.

54. Bhattacharjee, C.; Datta, S. (2003) Analysis of polarized layer resistance during ultrafiltration of PEG-6000: An approach based on filtration theory. *Sep. Purif. Technol.*, 33 (2): 115–126.